Master's Thesis

Development of catechol-based photocurable thermally conductive adhesives

Hyun Woo Choi

Department of Chemical Engineering

Graduate School of UNIST

2020

Development of catechol-based photocurable thermally conductive adhesives

Hyun Woo Choi

Department of Chemical Engineering

Graduate School of UNIST

Development of catechol-based photocurable thermally conductive adhesives

A thesis/dissertation
submitted to the Graduate School of UNIST
in partial fulfillment of the
requirements for the degree of
Master of Science

Hyun Woo Choi

06. 09. 2020
Approved by

Advisor
Dong Woog Lee

Development of catechol-based photocurable thermally conductive adhesives

Hyun Woo Choi

This certifies that the thesis/dissertation of Hyun Woo Choi is approved.

06. 09. 2020

signature

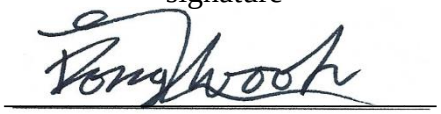

Advisor: Dong Woog Lee

signature

Hak-Sun Kim

signature

So Youn Kim

Abstract

Polymer composites are widely used as thermally conductive adhesives (TCAs) in electronic devices, owing to their high thermal conductivity and electrical resistance. However, while commercially available epoxy-based adhesives have good adhesive strength and thermal conductivity, they suffer from long curing times and particle aggregation at high filler loading levels, resulting in lower mechanical and thermal performance. Additionally, some thermoset polymers require high temperatures to fully cure, limiting their use in sensitive electronics. Photocurable TCAs have emerged as an alternative to thermoset adhesives because of their fast curing times at lower temperatures. However, these adhesives have not been able to match the mechanical and thermal performance of epoxy-based adhesives.

In this work, we developed photocurable and thermally conductive adhesives using catechol-based copolymers. The introduction of catechol-groups to the adhesive enables interactions with many surfaces through various adhesion mechanisms such as hydrogen bonding, π-π interactions, and cation-π interactions. The copolymers are synthesized using catechol, polyethylene glycol, and acrylate groups, which allow for highly adhesion, easy processing, and photocuring. Hexagonal boron nitride was used as the filler material due to its high thermal conductivity, excellent electrical insulation, high stability, and low cost. Additionally, we introduced conductive anthracene and pyrene functional groups to increase the thermal conductivity of the adhesive without the use of filler particles.

In Chapter 2, we tested the mechanical and thermal performance of various photocurable adhesives by measuring lap shear strength and thermal conductivity. A wide range of copolymer and adhesive compositions were utilized to investigate the effects of catechol functional groups on the lap shear strength of the adhesive. Boron nitride was added to the adhesive at various filler loads to study its effects on the performance of the adhesives.

In Chapter 3, we synthesized conductive monomers with anthracene and pyrene functional groups to improve the thermal conductivity of adhesives without the use of a thermally conductive filler. Generally, the thermal conductivity of a polymer adhesive is raised by adding filler particles. However, by incorporating conductive monomers into the adhesive, thermal conductivity was increased without using boron nitride particles.

Contents

Abstract----------v

Contents----------vii

List of Figures----------ix

List of Tables----------x

Chapter 1. Introduction----------1

Chapter 2. Catechol-based thermally conductive adhesives----------3

2.1 Experimental methods and materials----------3

2.1.1 Materials----------3

2.1.2 Preparation of catechol-based copolymers----------3

2.1.3 Preparation of adhesives----------5

2.1.4 Characterization----------5

2.2 Results and discussion----------6

2.2.1 Chemical compositions of copolymers----------6

2.2.2 Characterization of copolymers----------6

2.2.3 Chemical compositions of adhesives----------7

2.2.4 Characterization of adhesives----------8

2.2.5 Lap shear testing----------10

2.2.6 Thermal conductivity measurement----------12

2.3 Conclusion----------14

Chapter 3. Thermally conductive polymer matrix----------16

3.1 Experimental methods and materials----------16

3.1.1 Synthesis of 9-anthracenemethyl acrylate (mAt)----------16

3.1.2 Synthesis of 1-pyrenemethyl acrylate (mPy)----------16

3.2 Results and discussion----------17

3.2.1 Characterization of mAt----------17

3.2.2 Characterization of mPy----------18

3.2.3 Mechanical and thermal properties----------19

3.3 Conclusion----------20

Chapter 4. Summary----------22

References----------23

Acknowledgements----------26

List of Figures

Figure 2.1	Molecular structures of the monomers used to synthesize the polymer. (a) DMA, (b) PEG acrylate, (c) GMA, and (d) 4-hydroxybutyl acrylate	4
Figure 2.2	Acrylate functionalization of the synthesized copolymer (a) DPG to obtain (b) DPGa	4
Figure 2.3	^{1}H-NMR spectra of (a) DPG 181 and (b) DPGa 181	7
Figure 2.4	Molecular structures of the acrylate monomers used in the adhesive. (a) HDDA, (b) TA, and (c) Aa	8
Figure 2.5	TGA curves for D_1HT 154, D_1HT 334, and D_3HT 154 with h-BN loading levels of 50 wt%	9
Figure 2.6	DSC thermograms for D_1HT 334 and D_1HT 154 with h-BN loading levels of 50 wt%	10
Figure 2.7	Lap shear strengths of thermally conductive adhesives with 50 wt% h-BN filler	10
Figure 2.8	Lap shear strength of D_3HT 334 at various filler loading levels.	11
Figure 2.9	Density of D_3HT 334 at various filler loading levels	12
Figure 2.10	Thermal conductivity measurement of D_3HT 334 at various filler loading levels	14
Figure 3.1	Schematic diagram of the synthesis of (a) mPy and (b) mAt	16
Figure 3.2	(a) ^{1}H-NMR and (b) ^{13}C-NMR of mAt	17
Figure 3.3	(a) ^{1}H-NMR and (b) ^{13}C-NMR of mPy	18
Figure 3.4	Lap shear strength and thermal conductivity measurements of adhesives with conductive monomers. No h-BN filler was used in these tests.	20

List of Tables

Table 2.1 Chemical compositions of the acrylate monomers used to synthesize the polymer samples. All polymer samples include 4 mol% AIBN. The numbers represent the mol percent of the monomers before polymerization. 3

Table 2.2 Components used in the photocurable adhesives. All polymer samples include 1 wt% 2,2-dimethoxy-2-phenyl acetophenone as photoinitiator. The numbers represent the wt% of the components. 5

Table 2.3 Thermal conductivity values for adhesives at 50 wt% h-BN content. 13

Table 3.1 Composition of adhesives with conductive monomers. The names of some adhesives are changed to improve clarity. 19

Chapter 1. Introduction

Heat dissipation has become a critical issue in the performance of electronics because of the constant increase in performance and miniaturization of these devices. Without proper heat dissipation, electronic devices will perform poorly and undergo premature failure.[1,2] To address this problem, thermally conductive adhesives (TCAs) are used to aid in the transfer of heat between thermal surfaces.[3,4] Polymer adhesives are attractive due to their excellent electrical insulation, low cost, and ease of processability, but these adhesives suffer from low intrinsic thermal conductivity (0.1-0.3 W/m·K).[5] The conventional method to increase the thermal conductivity of polymer materials is to introduce thermally conductive fillers in order to form a polymer composite.[6,7]

A variety of these fillers including metals (Ag, 1-5.5 W m^{-1} K^{-1}), metal oxides (Al_2O_3, 0.8-2 W m^{-1} K^{-1}), metal nitrides (BN, 1-3.5 W m^{-1} K^{-1}), and graphene (1-16 W m^{-1} K^{-1})[11] are used to enhance the thermal conductivity of polymer composites. Among these fillers, hexagonal boron nitride (h-BN) stands out due to its electrical insulation, stability, low cost, and high thermal conductivity.[3] Another important aspect to consider is the filler content. While increasing the filler content in a TCA increases the thermal conductivity, high loading of filler particles in adhesives can lead to the degradation of mechanical properties and processability of a composite.

While epoxy-based thermoset composites can achieve filler loading levels of 80 wt%, the low processability of these composites causes the need for additional processing steps such as hot-pressing and surface modification of the fillers.[12,13] Epoxy-based composites become highly viscous at these loading levels, causing voids to form during the curing process. These voids not only affect the mechanical integrity of the adhesive, but also the thermal conductivity of the material.[6] Additionally, the long curing time of thermoset polymers can lead to the aggregation of filler particles and the high curing temperatures may prevent use in heat sensitive electronics.[14] Photocurable polymers can address these problems through their ability to rapidly cure at room temperature. However, adhesives using photocurable polymers have not been able to match the mechanical and thermal performance of epoxy composites. [15,16]

To improve the thermal conductivity of photocurable adhesives, phonon scattering sites need to be reduced. In polymer composites, phonon scattering primarily occurs between the filler particles and the polymer, so a strong interaction between these two is needed to reduce phonon scattering.[7] The ineffective distribution and aggregation of filler particles throughout the matrix is another cause of increased phonon scattering in polymer composites. Particle aggregation increases thermal interfacial

resistance between the filler particles and creates new sites for phonon scattering.[17] However, particle aggregation can be reduced through strong interactions between the polymer matrix and the filler particles. Due to the fast cure times of photocurable polymers, ensuring good dispersion of filler particles prior to curing can prevent the formation of particle aggregates.

While high thermal conductivities achieved through high filler content is desirable for some applications, other applications demand reduced filler loads.[6,18] Various methods to increase thermal conductivity at low filler loading levels have been explored. Some of these methods include: using magnetic or electric fields to align filler particles,[19] controlling the shape of the fillers through particle agglomeration,[12,20] and using fillers of differing sizes to maximize the contact area between fillers.[21] However, not a lot of research has been done on increasing the thermal conductivity of an adhesive without the use of thermally conductive fillers.

Since TCAs need to hold thermal surfaces together to aid in the transfer of heat, it is essential that the adhesive does not detach from the adherends. At a high filler content, a polymer adhesive will more readily detach from the adherends because of reduced contact with the surface, and it will have lower cohesion because of voids forming in the matrix.[6] To reduce the effects of high filler content on the adhesive, strong interactions between the adhesive and thermal surfaces are needed.

In this work, we synthesized a copolymer using catechol, polyethylene glycol, and acrylate groups to improve the mechanical strength of the adhesive and added hexagonal boron nitride as filler material to enhance the thermal conductivity of the composite. Catechol groups are well-known for their role in allowing mussel foot proteins to adhere to various surfaces through adhesion mechanisms such as hydrogen bonding, π-π interactions, and cation-π interactions.[22] The catechol groups allow the copolymer to strongly bind to h-BN particles, as well as to various surfaces. The polyethylene glycol groups improve the solubility and processability of the polymer, while the acrylate group enables the polymer's ability to be photocurable. Through the copolymer and h-BN particles, we developed a stable adhesive with high adhesion and thermal conductivity. By incorporating conductive monomers containing anthracene and pyrene groups into the adhesive, the adhesive's thermal conductivity was greatly enhanced without the use of fillers.

Chapter 2. Catechol-based thermally conductive adhesives

2.1 Experimental methods and materials

2.1.1 Materials

Poly(ethylene glycol) methyl ether acrylate (PEG acrylate, Mn = 480), acrylic acid (Aa, 99%), and glycidyl methacrylate (GMA, 97%) were purchased from Sigma. 4-hydroxybutyl acrylate (97%) and 2,2-dimethoxy-2-phenyl acetophenone were purchased from TCI. Azobis(isobutyronitrile) (AIBN) and triethyl amine (TEA, 99%) were purchased from Junsei. N,N-Dimethylformamide (DMF, 99.9%) and diethyl ether (99.8%) were purchased from Samchun. Hexane (98.5%) was purchased from SK Chemicals. 1,6-hexanediol diacrylate (HDDA, 99%) and trimethylolpropane triacrylate (TA) were purchased from Alfa Aesar. Hexagonal boron nitride (h-BN, SGPS grade, 13.7 μm) was purchased from Denka.

2.1.2 Preparation of catechol-based copolymers

Polymers	DMA	PEG acrylate	GMA
DPG 181	10	80	10
DPG 172	10	70	20
DPG 163	10	60	30
DPG 262	20	60	20
DPG 352	30	50	20
DPG 442	40	40	20

Table 2.1 Chemical compositions of the acrylate monomers used to synthesize the polymer samples. All polymer samples include 4 mol% AIBN. The numbers represent the mol percent of the monomers before polymerization.

The copolymer was synthesized from the free radical solution polymerization of DOPA methacrylate (DMA), PEG acrylate, and GMA (Fig. 2.1). The polymerization of these monomers was done in a two-neck round flask. A solution containing 10 mol of the monomers (Table 2.1) in DMF (11 ml) was added to the flask. The flask was placed in an 80 °C oil bath while stirring the solution until the solution reached a constant temperature. The solution was exposed to a nitrogen atmosphere before adding 4 mol% of AIBN initiator dissolved in 1 ml of DMF. After a 1-hour reaction with constant stirring, the polymer was precipitated in a 1:1 hexane to diethyl ether solution. After removing the excess solvent,

the polymer was dissolved in DMF (5 ml) and stirred until fully dissolved. 4-hydroxybutyl acrylate and TEA were added to the solution in excess quantities of the GMA used to synthesize the copolymer. After a 4-hour reaction with constant stirring, the acrylate functionalized polymer was precipitated in a 1:1 hexane to diethyl ether solution.

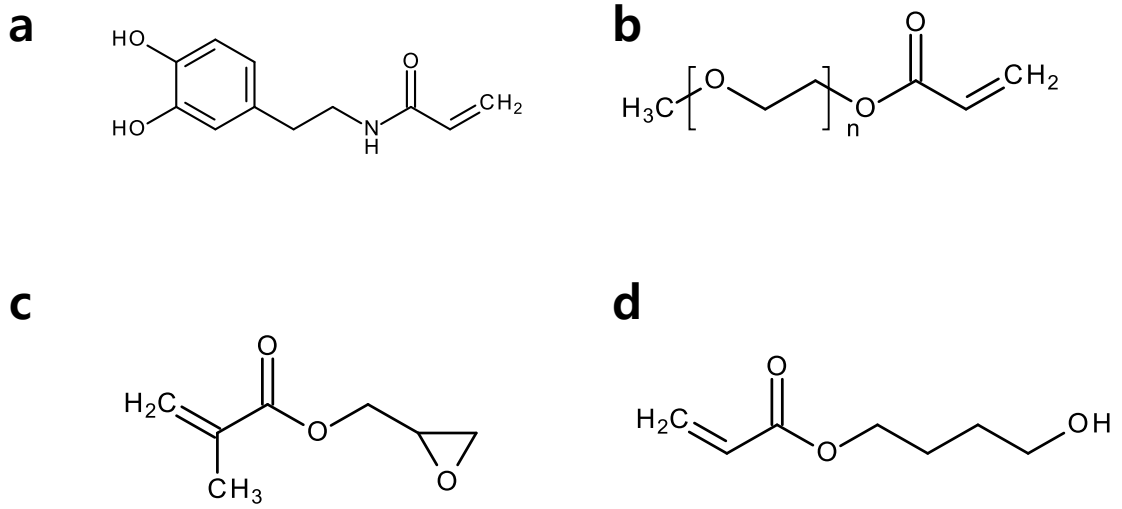

Figure 2.1 Molecular structures of the monomers used to synthesize the polymer. (a) DMA, (b) PEG acrylate, (c) GMA, and (d) 4-hydroxybutyl acrylate

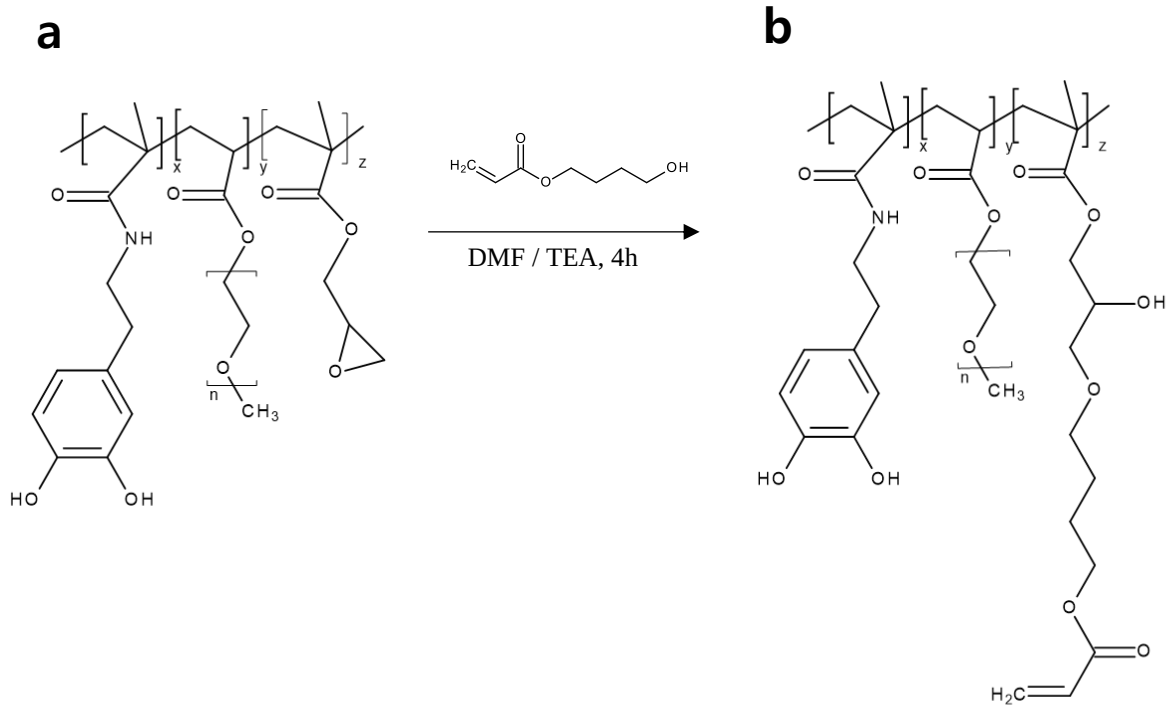

Figure 2.2 Acrylate functionalization of the synthesized copolymer (a) DPG to obtain (b) DPGa

2.1.3 Preparation of adhesives

Adhesive	DPGa 172	DPGa 262	DPGa 352	HDDA	TA	Aa
D_1H 19	10			90		
HT 64				60	40	
D_1HT 154	10			50	40	
D_1HT 244	20			40	40	
D_1HT 334	30			30	40	
D_2HT 154		10		50	40	
D_2HT 244		20		40	40	
D_2HT 334		30		30	40	
D_3HT 154			10	50	40	
D_3HT 244			20	40	40	
D_3HT 334			30	30	40	
D_3AT 334			30		40	30

Table 2.2 Components used in the photocurable adhesives. All polymer samples include 1 wt% 2,2-dimethoxy-2-phenyl acetophenone as photoinitiator. The numbers represent the wt% of the components.

The catechol-based copolymers DPGa 172, DPGa 262, and DPGa 352 were used in the adhesives. These copolymers were mixed with the acrylate monomers HDDA, TA, and Aa in the weight percentages described in Table 2.2. The photoinitiator, 2,2-dimethoxy-2-phenyl acetophenone, was then dissolved in the prepolymer and crosslinker mixture. The desired amount of h-BN filler particles was added to the adhesive mixture, and the adhesive was thoroughly mixed with a vortex device prior to use.

2.1.4 Characterization

The lap shear testing of the adhesives was conducted using a universal testing machine (WL2100C, Withlab, South Korea). The lap shear testing was done in accordance with ASTM D3163 using PMMA adherends, although the dimensions of the adherends were modified to accommodate for the strength of the adhesive. Proton nuclear magnetic resonance (^{1}H-NMR) spectra using $CDCl_3$ as the solvent were

recorded on a Bruker 400 MHz FT-NMR, AVANCE III HD. An Agilent 1260 Infinity II gel permeation chromatography (GPC) system was used to measure the molecular weight of the polymers using THF as the eluent. Differential scanning calorimetry (DSC) was done on a TA Instruments Inc. Q200 DSC system. About 5 mg of a polymer composite sample was tested in the range of -20—140 °C or -20—200 °C for thermal conductivity calculations and glass transition temperature analysis, respectively, with ramp rates of 10 °C/min. The heating cycle was repeated two times, and the second heating cycle was used in thermal conductivity calculations. A TA Instruments, Inc. Q500 TGA system was used to perform thermogravimetric analysis (TGA) of the polymer composites. Samples of about 10 mg were heated from 40—600 °C under a nitrogen atmosphere with a ramp rate of 10 °C/min. The thermal diffusivities of the polymer composites were measured with a Linseis XFA 300 laser flash analyzer at room temperature.

2.2 Results and discussion

2.2.1 Chemical compositions of copolymers

While a copolymer with high mol% of DMA and GMA is desired to achieve high adhesion strength and crosslinking ability, too little PEG acrylate content in the copolymer can cause it to undergo gelation, rendering it insoluble and difficult to process. To optimize the composition of the polymer, DPG 181 was used as a baseline for making variations to the copolymer composition. First, the GMA content was increased from 10 mol% in DPG 181 to 20 mol% and 30 mol% in the DPG 172 and DPG 163 copolymers, respectively. While DPG 181 and DPG 172 remained stable, DPG 163 experienced gelation within a few days. Since GMA could only be increased to about 20 mol% before the polymer became unstable, this mol ratio for GMA was maintained in the other copolymers. The mol% of DMA was also incrementally increased up to 40 mol%, at which point the copolymer became a solid when the solvent was removed. The remaining stable copolymers (DPG 172, DPG 262, and DPG 352) were reacted with 4-hydroxybutyl acrylate to attach an acrylate functional group. After acrylate functionalization, DPGa 172, DPGa 262, and DPGa 352 were obtained. These copolymers were able to remain stable for prolonged periods and were used to study the effect of catechol content on adhesion strength.

2.2.2 Characterization of copolymers

The chemical structure of the copolymer was analyzed using ^{1}H-NMR spectroscopy (Fig 2.3). Two aromatic peaks for catechol appear at 6.6 and 6.7-6.8 ppm. After acrylate functionalization of the polymer, acrylate peaks appear at 5.9 and 6.4-6.5 ppm. These results indicate that DMA and GMA were successfully copolymerized, and the acrylate functionalization of the polymer was successful. The

number average molecular weight (Mn) of DPG 172 was 10,854 g/mol, which is around the expected value.

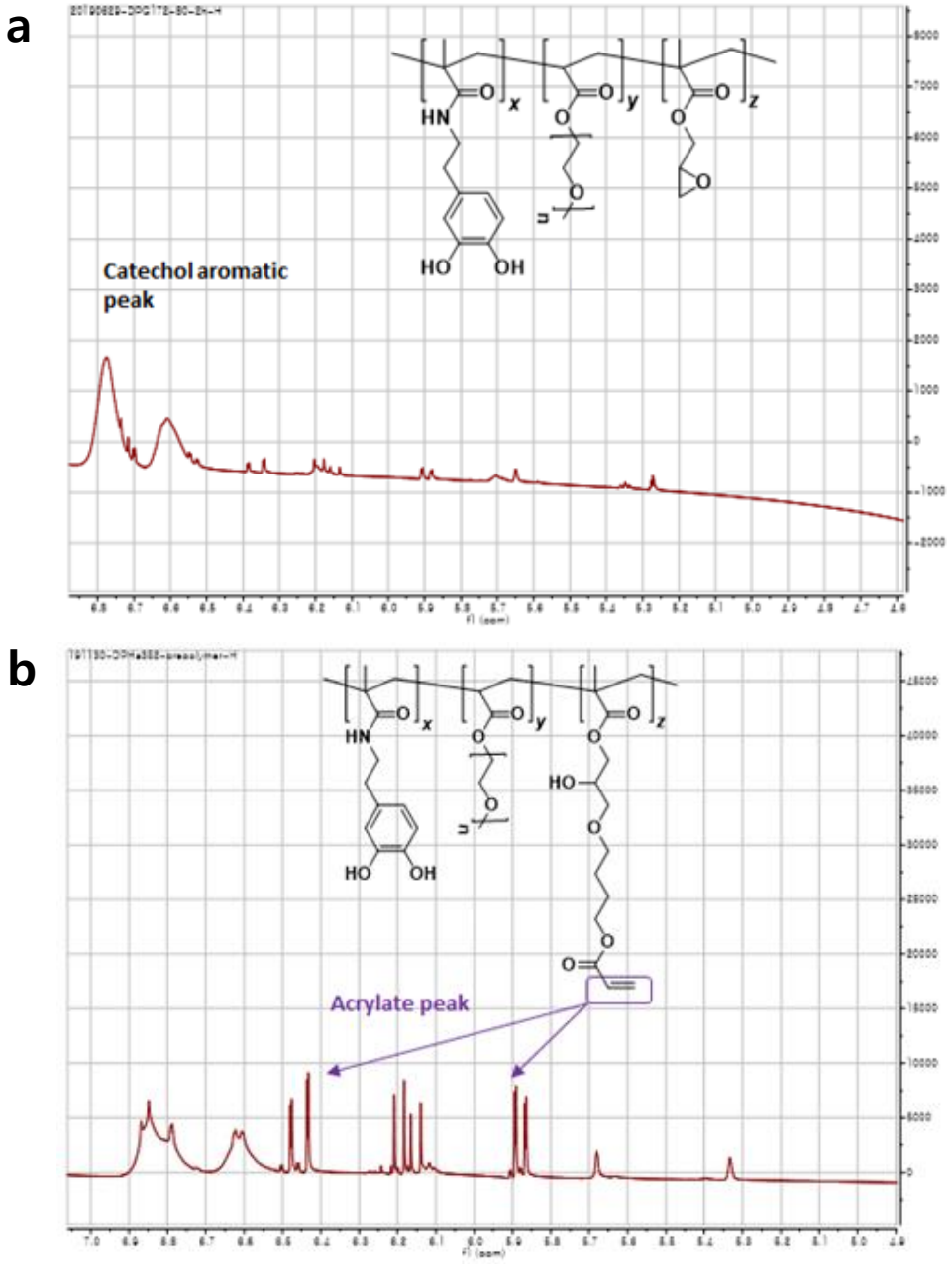

Fig. 2.3 ^{1}H-NMR spectra of (a) DPG 181 and (b) DPGa 181

2.2.3 Chemical compositions of adhesives

The main components of the adhesives are DPGa, the acrylate monomers (Fig. 2.4), and h-BN filler. DPGa improves the adhesion strength of the composite through strong interactions between the catechol groups in the polymer and the surfaces that the adhesive is bound to. The multiple acrylate groups in

HDDA and TA, allow these acrylates to act as crosslinkers in the adhesive mixture. Additionally, these crosslinkers are known to have some adhesive properties.[23,24] While TA showed higher adhesion strength than HDDA, raising the amount of TA in the adhesive above 40 wt% causes the viscosity of the adhesive to be too high to increase h-BN content to the desired value (80 wt%), so HDDA is used to lower the viscosity of the adhesive sample while still being able to perform as a crosslinker. D_1H 19 was used to confirm the higher adhesion strength of TA compared to HDDA, and HT 64 was used to better understand the adhesive properties of catechol.

To understand the effects of the catechol group on adhesive strength, the copolymers DPGa 172, DPGa 262, and DPGa 352 were used as components in the adhesives. The wt% of the polymers was increased from 10 to 30 wt%, as samples containing 40 wt% or more of the polymer were too viscous to increase h-BN content to 80 wt%.

In D_3AT 334, HDDA is replaced with acrylic acid to increase the lap shear strength of the adhesives. Acrylic acid was incorporated into the adhesive to introduce carboxylic groups, which are capable of hydrogen bonding, and to decrease the crosslinker ratio, which should enhance adhesion strength.[25–28]

2.2.4 Characterization of adhesives

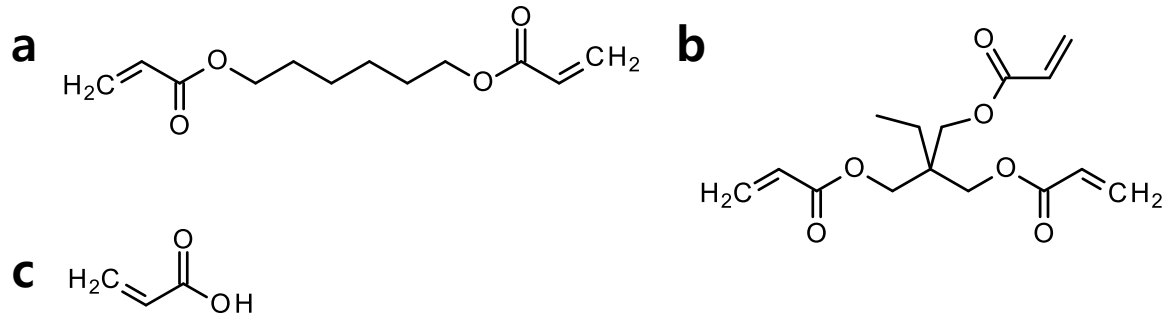

Figure 2.4 Molecular structures of the acrylate monomers used in the adhesives. (a) HDDA, (b) TA, and (c) Aa

Since thermally conductive adhesives can be exposed to high temperatures while helping to transfer excess heat away from electronics, it is crucial that they remain stable at these temperatures and do not degrade. Thermal degradation of TCAs affects both the structural integrity and the thermal conductivity of the adhesive. When the polymer matrix in the composite degrades, the filler network is damaged and contact between the filler particles is disturbed, increasing the number of phonon scattering sites.[29] As shown in Fig. 2.5, the D_1HT 154 adhesive with 50 wt% h-BN content showed slight degrading around 100 °C, and reached the 5% thermal degradation temperature (T_{5d}) at 350 °C. The degradation of the adhesive around 100 °C is thought to occur because of the incomplete curing of the adhesives, which leaves some monomers that degrade at around 100 °C. However, by increasing the DPGa 172 content

in the adhesive to 30 wt%, little to no degradation was observed until temperatures above 300 °C. Adhesives containing DPGa polymers with higher DMA mol ratios such as DPGa 352 also did not experience significant degradation until temperatures above 300 °C. The T_{5d} values for D_1HT 334 and D_3HT 154 are 380 °C and 390 °C, respectively. Lastly, the 3 adhesives rapidly degraded between 400-475 °C, down to a weight of about 40% of the original weight. This remaining weight is from the h-BN particles, since these particles remain stable until temperatures above 1000 °C.[30]

Another important aspect of the thermal stability of TCAs is the glass transition temperature (T_g). TCAs need to have a T_g that is higher than the temperatures reached by the surfaces it is in contact with, to prevent the transition to a rubbery state. The DSC thermograms of D_1HT 244 and D_3HT 154 show no T_g in the range of -20 °C to 140 °C (Fig 2.6). The DSC thermogram for D_1HT 154 is not shown due to the partial degradation of the adhesive at around 100 °C, as seen in the TGA curves. Since the polymer matrix becomes highly crosslinked and rigid when fully cured, the T_g does not exist in the expected operating range of thermally conductive adhesives.

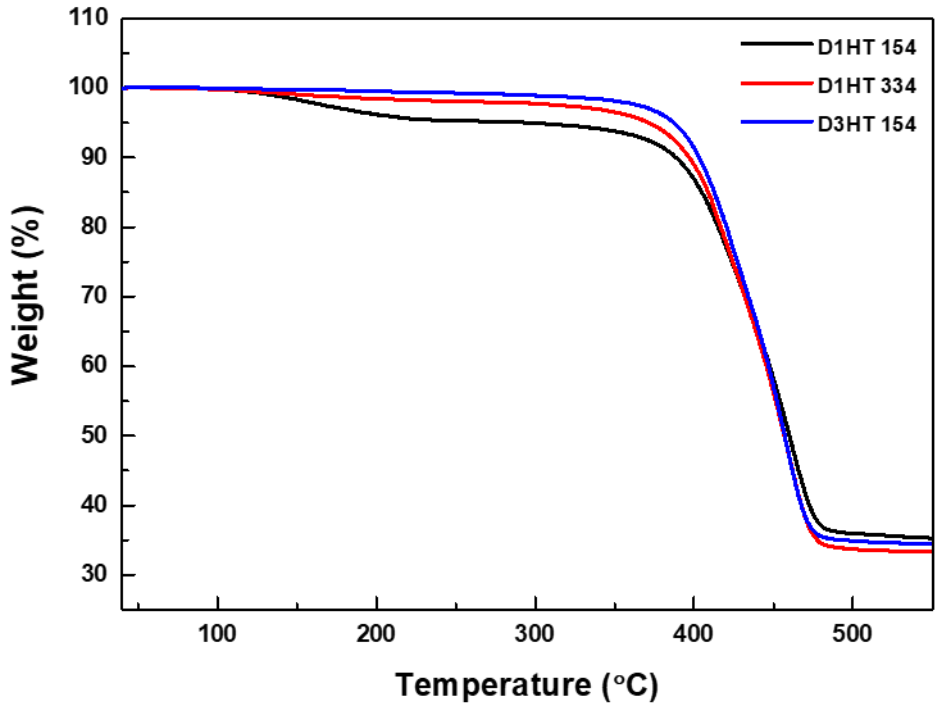

Fig. 2.5 TGA curves for D_1HT 154, D_1HT 334, and D_3HT 154 with h-BN loading levels of 50 wt%

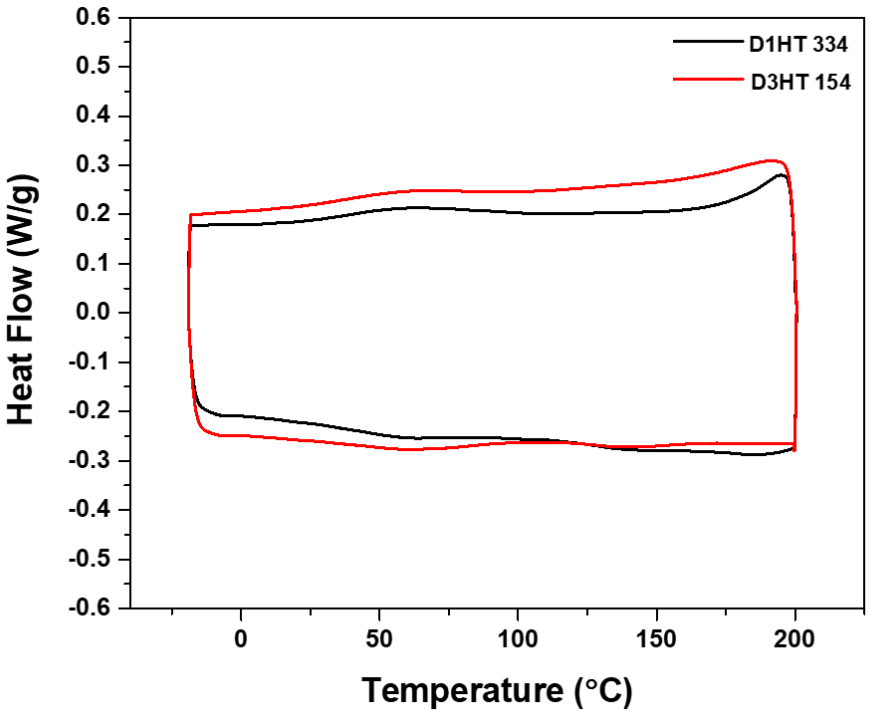

Fig. 2.6 DSC thermograms for D_1HT 334 and D_1HT 154 with h-BN loading levels of 50 wt%

2.2.5 Lap shear testing

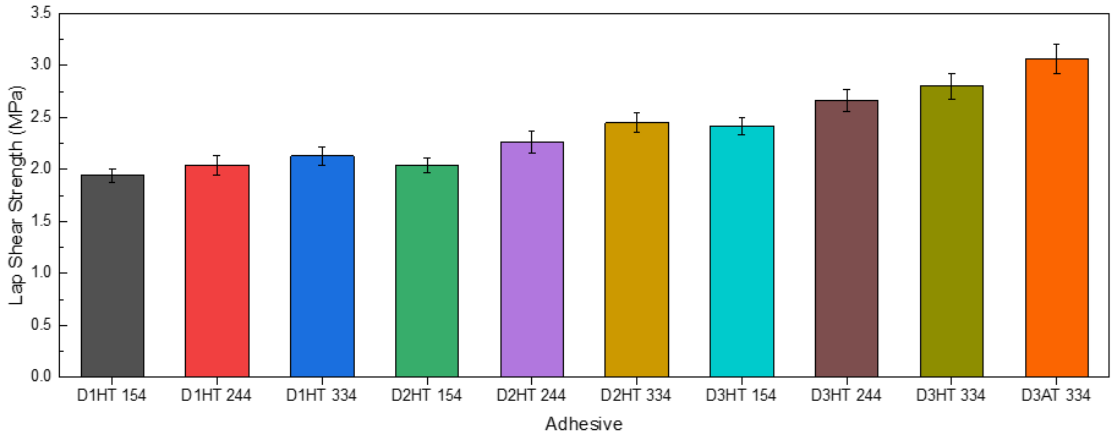

Fig. 2.7 Lap shear strengths of thermally conductive adhesives with 50 wt% h-BN filler

Single lap shear tests of the adhesives between two PMMA adherends were done to characterize the adhesion strength of the thermally conductive adhesives. All the joints in the lap shear tests had an adhesive failure mode. PMMA was used as the adherend material due to its transmittance of UV light, which was necessary for curing the adhesives. The effects of each component on adhesion was observed through variations in the adhesive composition. To understand the effect of TA on lap shear strength, D_1HT 19 and D_1HT 154 are compared. The difference between the two adhesives is the substitution of 40 wt% TA in D_1HT 154 with 40 wt% HDDA in D_1H 19. The lap shear strength of D_1H 19 was about

32% lower than that of D_1HT 154, which confirmed the higher adhesion strength of TA. The amount of TA in the adhesives was kept at 40 wt% for all remaining adhesives.

Using D_1HT 154 as a baseline, we replaced the catechol-based prepolymer with HDDA crosslinker to observe the effects of the catechol on lap shear strength. This resulted in a 12% decrease in lap shear strength relative to D_1HT 154, confirming the strong adhesive properties of the synthesized copolymer. The strength of the adhesive could be enhanced by increasing the polymer content in the adhesive. As shown in Fig. 2.7, the lap shear strength of adhesives with DPGa 172 increased with increasing polymer ratios. Adhesive strength also increased when DPGa 172 was substituted with the other copolymers with a higher catechol content, DPGa 262 and DPGa 352. The D_3HT 334 adhesives had a lap shear strength of 2.80 MPa, which was about 44 % higher than that of D_1HT 154.

To increase the lap shear strength of the adhesives even further, Aa was used to substitute HDDA in the adhesive. D_3AT 334 had the highest lap shear strength of adhesives with 50 wt% h-BN content. This increase in lap shear strength compared to D_3HT 334 is caused by the carboxylic groups, which are capable of hydrogen bonding, and the lower crosslinking ratio, which was achieved by replacing HDDA.[25–28]

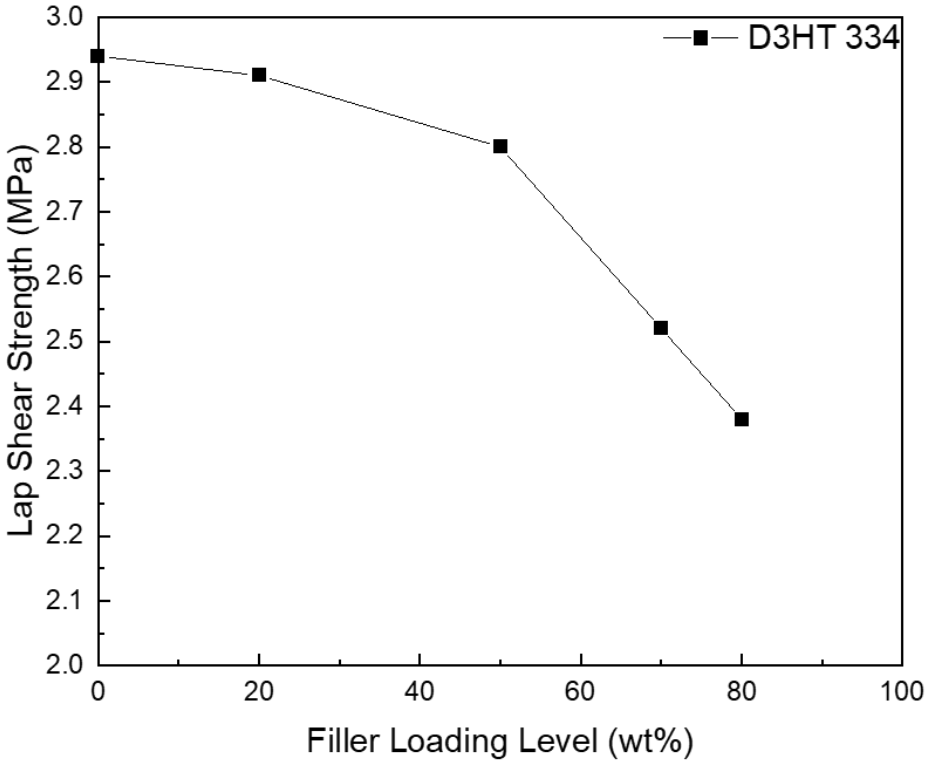

Fig. 2.8 Lap shear strength of D_3HT 334 at various filler loading levels.

Fig. 2.8 shows the lap shear strength of D_3HT 334 at various h-BN loading levels. The decrease in lap shear strength up to 50 wt% h-BN content is low, with a decrease of 5% in adhesion strength compared to D_3HT 334 adhesive without filler. However, lap shear strength sharply decreases after that point. At 80 wt% h-BN content, the lap shear strength had decreased by 20% relative to the adhesive without filler. This sudden decrease in lap shear strength after 50 wt% h-BN filler occurs because of poor filler dispersion and void formation in the adhesive.[31–33] Due to the sharp increase in viscosity of the adhesive before curing at 70 wt% and 80 wt% filler content, the h-BN particles could not be dispersed well enough to avoid some particle aggregation before curing. Additionally, void formation also occurs at higher viscosity, since the air that gets trapped during the filler mixing step becomes harder to remove.[31]

2.2.6 Thermal conductivity measurement

The thermal conductivity of the TCAs was calculated using thermal diffusivity data obtained by laser flash analysis using the equation $k = \alpha \rho c_p$, where k is the thermal conductivity, α is the thermal diffusivity, ρ is the sample density, and c_p is the specific heat capacity of the sample. Due to the good distribution of h-BN fillers throughout the polymer matrix from 0 wt% to 50 wt%, the density of the adhesive increases almost linearly with filler loading level (Fig 2.9). However, the density at filler loads of 70 wt% and 80 wt% slightly deviated from the trend. This appears to be in good accord with the lap shear data at these filler loads, suggesting that particle aggregation and void formation have a noticeable effect on the density of adhesives at high filler contents. In contrast, filler loading level does not have a significant effect on the specific heat capacity of the adhesives, so changes to the thermal conductivity of adhesives that occur by changing filler loading levels can be attributed to the higher density and thermal diffusivity of the TCAs.

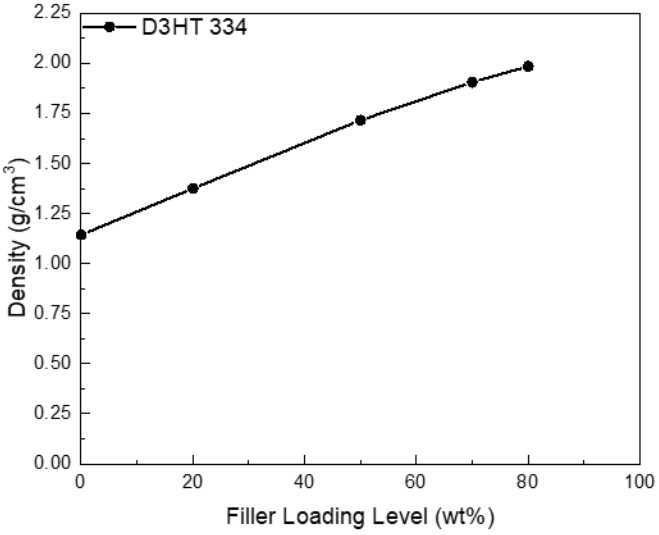

Fig. 2.9 Density of D_3HT 334 at various filler loading levels

The thermal conductivity of polymer composites is known to come primarily from the thermally conductive fillers since most polymers have very low thermal conductivities.[3] Assuming that the fillers are well dispersed and the filler content is the same, the thermal conductivity values of adhesives with different compositions are expected to have similar values. The results in Table 2.3 show that at a filler content of 50 wt%, all the adhesives tested have thermal conductivity values around 2 W/m·K. Since the composition does not appear to have a significant effect on the thermal conductivity values of the adhesives, thermal conductivity measurements were performed on a single adhesive, D_3HT 334.

Fig. 2.10 shows thermal conductivity measurements of D_3HT 334 taken at h-BN loads from 0 wt% to 80 wt% At an h-BN content of 0 wt%, the adhesive shows a very low thermal conductivity of 0.26 W/m·K, which is characteristic of acrylate adhesives. The thermal conductivity of the adhesive increases up to 3.42 W/m·K at an h-BN content of 80 wt%. However, the rate of increase in thermal conductivity with respect to filler load between 70 wt% and 80 wt% filler content was noticeably lower than the rate between 0 wt% and 70 wt% h-BN, which is caused by particle aggregation and void formation. Particle aggregation lowers the thermal conductivity of the adhesive by introducing new phonon scattering sites, and voids in the adhesive increase its thermal resistivity due to the air trapped inside.[6,29] While some particle aggregation and void formation is believed to occur at 70 wt% h-BN content, according to the lap shear data and density measurement, the thermal conductivity of the adhesive does not appear to have been greatly affected.

Adhesive	Thermal Conductivity (W/m·K)
D_1HT 154	2.05
D_1HT 244	1.90
D_1HT 334	1.99
D_2HT 154	2.10
D_2HT 244	2.05
D_2HT 334	2.08
D_3HT 154	2.01
D_3HT 244	2.01
D_3HT 334	1.97

Table 2.3 Thermal conductivity values for adhesives at 50 wt% h-BN content.

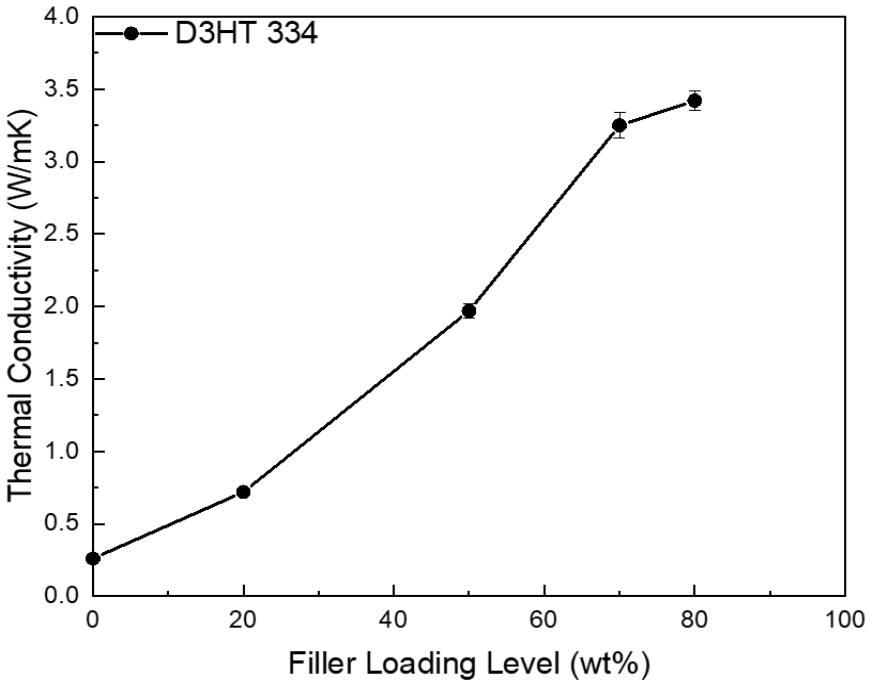

Fig. 2.10 Thermal conductivity measurement of D_3HT 334 at various filler loading levels

2.3 Conclusion

Catechol-based polymer adhesives were synthesized by the copolymerization of DMA, PEG acrylate, and GMA, and they were later functionalized with an acrylate group that enabled the copolymer to be photocurable when added to the adhesive mixture. The catechol functional group in DMA enhances the adhesion strength of the copolymer, while PEG acrylate makes the copolymer soluble and easy to process. The copolymer was characterized by ^{1}H-NMR spectra, which showed aromatic peaks from the catechol group in DMA and acrylate peaks after the copolymer's reaction with 1,4-hydroxybutyl acrylate. Additionally, the chemical composition of the polymer was optimized by modifying the DMA and GMA mol ratios while reducing PEG acrylate to obtain three stable copolymers: DPGa 172, DPGa 262, and DPGa 352. The catechol-based copolymers were mixed with acrylate crosslinkers (HDDA and TA) and hexagonal boron nitride particles to make thermally conductive adhesives. These adhesives showed excellent thermal stability, with 5% thermal degradation temperatures above 350 °C and no glass transition temperature in the range of -20~200 °C. Lap shear test results show that an increase in the amount of catechol functional groups present in the adhesive increases the lap shear strength of the adhesive. The strength of the adhesives was seen to increase when increasing the wt% of DPGa in the adhesive and when using DPGa polymers with a higher catechol content (DPGa 352). The lap shear strength of the polymer was further increased by replacing some of the crosslinker with acrylic acid.

Through these optimizations, D_3AT 334 was able to reach a lap shear strength of 3.06 MPa at 50 wt% h-BN content. However, lap shear strength decreased with increasing filler content. At 70 wt% and 80 wt% filler loads, there was a sharp decrease in lap shear strength. Thermal conductivity measurement results showed that adhesive composition did not have a significant effect on thermal conductivity since all adhesive samples had thermal conductivities of around 2 W/m·K at 50 wt% h-BN load. However, increasing filler content affects thermal conductivity by increasing density and thermal diffusivity of the adhesive. At a filler load of 80 wt%, the thermal conductivity of D_3HT 334 was 3.42 W/m·K. The development of these highly adhesive and thermally conductive photocurable polymer composites is expected to contribute towards the development of alternatives for epoxy-based thermally conductive adhesives.

Chapter 3. Thermally conductive polymer matrix

3.1 Experimental methods and materials

Polymer synthesis, ^{1}H-NMR spectroscopy, lap shear test, and thermal conductivity measurements were conducted according to the experimental methods described in 2.1 Experimental methods and materials.

3.1.1 Synthesis of 9-anthracenemethyl acrylate (mAt)

2.00 g of 9-hydroxymethyl anthracene was added to a two-neck round flask. After degassing the flask, 30 ml of anhydrous tetrahydrofuran (THF) was added, and the solution was purged with argon gas for 5 min. 4.01 ml of triethylamine was then added to the solution. An ice bath was used to cool the solution while 2.34 ml of acryloyl chloride was added to the solution dropwise over a few minutes. The reaction proceeded for 3 hours while the solution was constantly stirred at room temperature. The product was extracted with diethyl ether, and the organic layer was washed with 1 M HCl and brine. This layer was then dried with $MgSO_4$. Excess solvent was removed, and the remaining solution was purified with a flash column (hexane : AcOEt = 4 : 1).

3.1.2 Synthesis of 1-pyrenemethyl acrylate (mPy)

2.00 g of 1-pyrenemethanol was added to a two-neck round flask. After degassing the flask, 30 ml of anhydrous tetrahydrofuran (THF) was added, and the solution was purged with argon gas for 5 min. 3.60 ml of triethylamine was then added to the solution. An ice bath was used to cool the solution while 2.17 ml of acryloyl chloride was added to it dropwise over a few minutes. The reaction proceeded for 3 hours while the solution was constantly stirred at room temperature. The product was extracted with diethyl ether, and the organic layer was washed with 1 M HCl and brine. This layer was then dried with $MgSO_4$. Excess solvent was removed, and the remaining solution was purified with a flash column (hexane : AcOEt = 4 : 1).

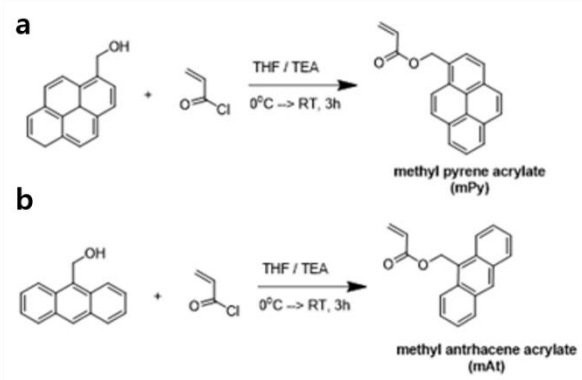

Fig. 3.1 Schematic diagram of the synthesis of (a) mPy and (b) mAt

3.2 Results and discussion

3.2.1 Characterization of mAt

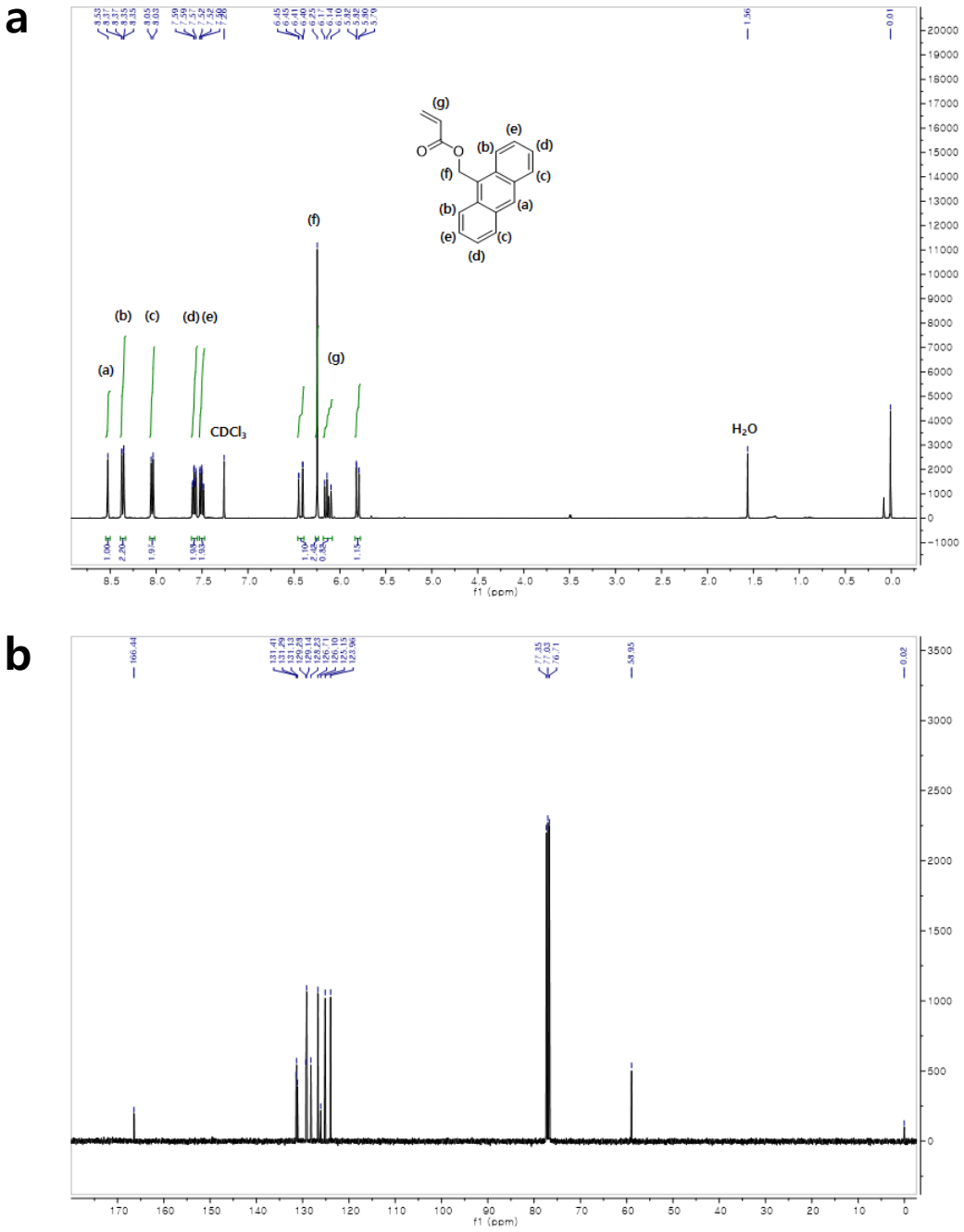

Fig. 3.2 (a) ^{1}H-NMR and (b) ^{13}C-NMR of mAt

^{1}H NMR: 8.53 (s, 1H), 8.37 (d, 2H, 8.0Hz), 8.05 (d, 2H, 8.0Hz), 7.56 (m, 4H), 6.42 (dd, 1H), 6.25 (s, 2H), 6.14 (dd, 1H), 5.81 (dd, 1H) ; ^{13}C NMR (ppm, $CDCl_3$, 100 MHz, δ): 166.44, 134.41, 131.29,

131.13, 129.28, 129.14, 128.23, 126.71, 126.10, 125.15, 123.96, 58.95 ; Mass : exact mass 262.10, found 262.1. The aromatic peaks of the product appear between 7.5 and 8.5 ppm (Fig. 3.1).

3.2.2 Characterization of mPy

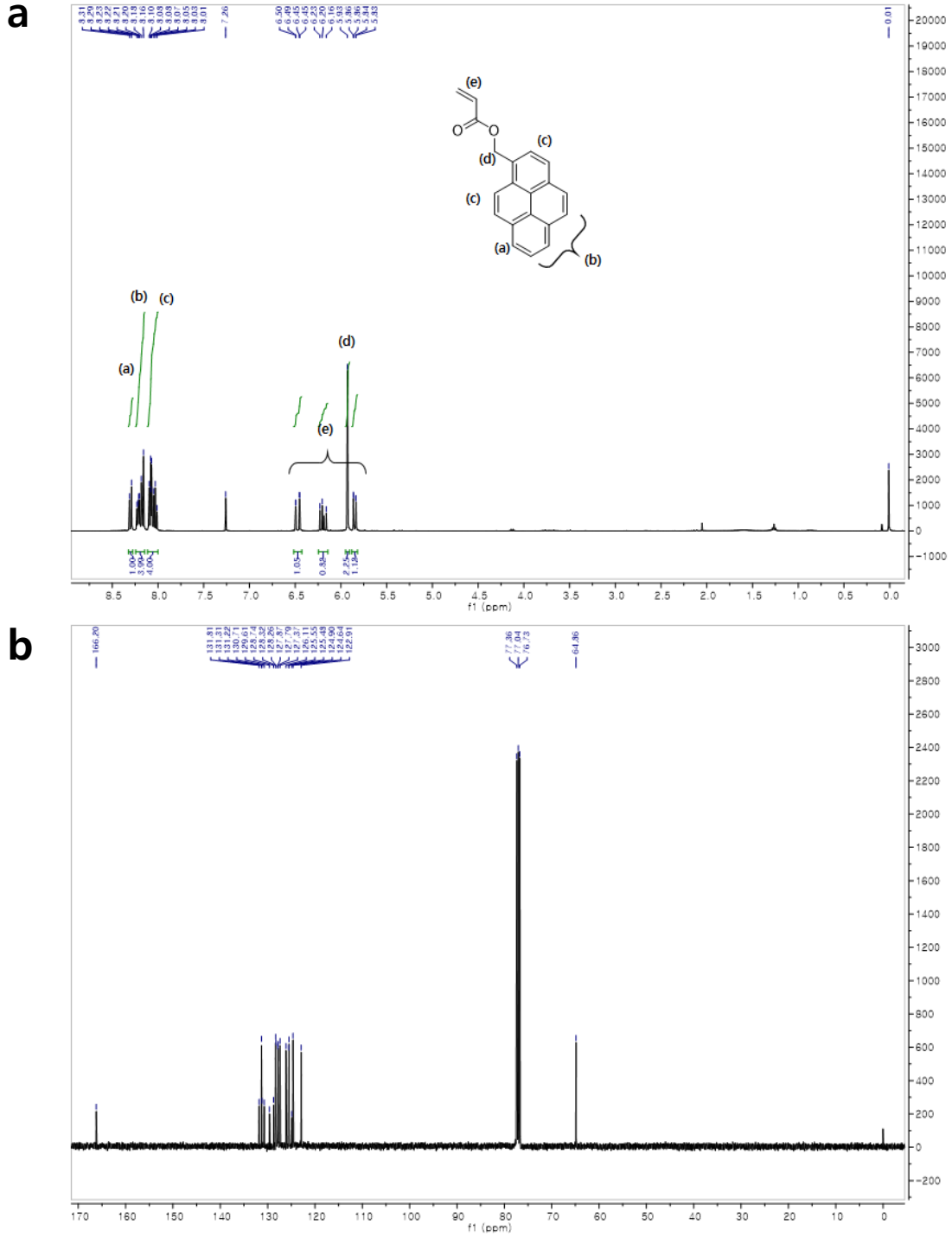

Fig. 3.3 (a) ^{1}H-NMR and (b) ^{13}C-NMR of mPy

^{1}H NMR: 8.53 (s, 1H), 8.37 (d, 2H, 8.0Hz), 8.05 (d, 2H, 8.0Hz), 7.56 (m, 4H), 6.42 (dd, 1H), 6.25 (s,

2H), 6.14 (dd, 1H), 5.81 (dd, 1H) ; ^{13}C NMR (ppm, $CDCl_3$, 100 MHz, δ): 166.44, 134.41, 131.29, 131.13, 129.28, 129.14, 128.23, 126.71, 126.10, 125.15, 123.96, 58.95 ; Mass : exact mass 262.10, found 262.1. The aromatic peaks of the product appear in a narrower range between 8.0 and 8.5 ppm (Fig. 3.2).

3.2.3 Mechanical and thermal properties

Adhesive	DPGa 352	HDDA	Aa	TA	mAt	mPy
A1	30	30		40		
A2	30	20		40	10	
A3	30	20		40		10
A4	30	10		40	20	
A5	30	10		40		20
B1	30		30	40		
B2	30		20	40	10	
B3	30		20	40		10
B4	30		10	40	20	
B5	30		10	40		20

Table 3.1 Composition of adhesives with conductive monomers. The names of some adhesives are changed to improve clarity.

The conductive monomers, mAt and mPy, were integrated into the adhesives to improve thermal conductivity without the addition of conductive fillers. Using the A1 adhesive (same as D_3HT 334 in Chapter 2) as a base, mAt and mPy were incorporated by substitution of HDDA in different weight percentages to obtain adhesives A2 – A5. Likewise, using the B1 adhesive (same as D_3AT 334 in Chapter 2) as a base, mAt and mPy substituted HDDA in different weight percentages to obtain the adhesives B2 – B5.

In adhesives A2 – A5 and B2 – B5, the increase in weight ratio of mAt and mPy resulted in a slight decrease in lap shear strength compared to A1 and B1, respectively (Fig. 3.4). Although crosslinking ratio is reduced since the conductive monomers substitute HDDA, the low adhesive strength of the anthracene and pyrene groups cancels out the benefits of lower crosslinking.

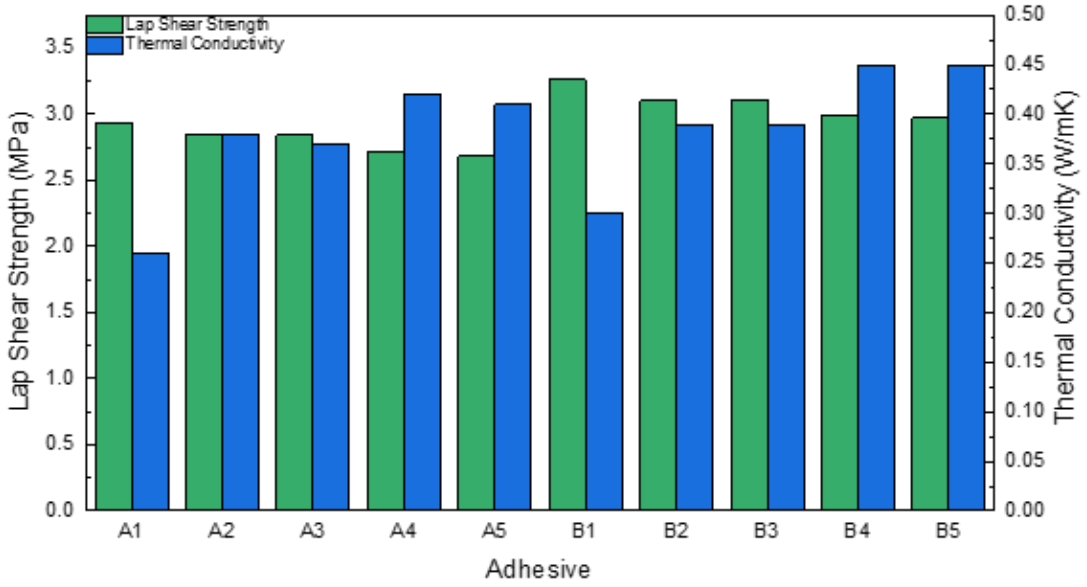

Fig. 3.4 Lap shear strength and thermal conductivity measurements of adhesives with conductive monomers. No h-BN filler was used in these tests.

While lap shear strength was not greatly affected by the use of conductive monomers in the adhesive, the thermal conductivity of the adhesives was greatly increased. In adhesives with 10 wt% mAt or mPy, the thermal conductivity increased from 0.26 W/m·K to 0.38 W/m·K and 0.37 W/m·K in A2 and A3, respectively. Further increasing the mAt and mPy content to 20 wt%, the thermal conductivity increased up to 0.42 W/m·K and 0.41 W/m·K in A4 and A5, respectively. The conductive monomers are able to increase the thermal conductivity of the adhesive through π- π stacking interactions, where the aromatic rings can enable phonon transport in the adhesive.[34] Additionally, B1-B5 have higher thermal conductivities than A1-A5. Acrylic acid is also to increase the thermal conductivity of the adhesives as a result of hydrogen bonding.[35] Through this, a thermal conductivity of 0.45 W/m·K was achieved in adhesives B4 and B5. Increasing the conductive monomer content of the adhesives past 20 wt% is expected to further increase thermal conductivity.

3.3 Conclusion

The conductive monomers, mAt and mPy were synthesized and incorporated into the catechol-based polymer adhesives. To confirm the successful synthesis of mAt and mPy, the conductive monomers were analyzed by ^{1}H-NMR and ^{13}C-NMR spectra. The ^{1}H-NMR spectra for both mAt and mPy showed

aromatic peaks corresponding to the anthracene and pyrene groups and peaks corresponding to the acrylate groups. The adhesives incorporating the conductive monomers showed a slight decrease in lap shear strength despite the conductive monomers reducing the crosslinking ratio through the substitution of HDDA. Lap shear strength decreased with increasing conductive monomer content in the adhesive because of the low adhesion strength of the mAt and mPy functional groups. Although lap shear strength decreased, thermal conductivity greatly increased in adhesives containing the conductive monomers because of their ability to enhance phonon transport in the polymer. Acrylic acid was also able to enhance the thermal conductivity of the adhesives by introducing additional groups capable of hydrogen bonding. This research is expected to help improve the thermal conductivity of adhesives without the use of conductive fillers, and higher conductive monomer content is expected to further increase thermal conductivity.

Chapter 4. Summary

In this work, we developed catechol-based photocurable adhesives with high adhesion and thermal conductivity. Copolymers were synthesized with DMA, PEG acrylate, and GMA monomers to improve adhesion and processability, and the copolymers were functionalized with an acrylate group to ensure that the copolymer was photocurable. Adhesives that incorporated the copolymers showed good thermal stability, with high thermal degradation temperatures above 350 °C.

The mechanical and thermal performance of the adhesives was analyzed through their lap shear strength and thermal conductivity. The lap shear strength of the adhesives improved with increased catechol content in the adhesive. Catechol content was increased by raising the content of the copolymers in the adhesive and using copolymers with higher catechol ratios. To further increase adhesive strength, acrylic acid was used to substitute the crosslinker, HDDA. The increase in hydrogen bonding groups coupled with the reduction of crosslinking ratio enhanced the lap shear strength of the adhesive. Through the addition of h-BN fillers to the adhesive, thermal conductivity was increased. The filler loading level was increased from 0 wt% to 80 wt%, and the highest thermal conductivity was obtained at 80 wt% h-BN. However, lap shear strength decreased at high filler loads.

In order to increase thermal conductivity without the use of fillers, conductive monomers (mAt and mPy) were synthesized and incorporated into the adhesive. Adhesives that incorporated these conductive monomers had significantly higher thermal conductivity without much loss in lap shear strength compared to adhesives with no conductive functional groups. Additionally, adhesives with acrylic acid had higher thermal conductivities due to the presence of the carboxylic groups which are capable of hydrogen bonding.

References

(1) Chen, J.; Huang, X.; Zhu, Y.; Jiang, P. Cellulose Nanofiber Supported 3D Interconnected BN Nanosheets for Epoxy Nanocomposites with Ultrahigh Thermal Management Capability. *Adv. Funct. Mater.* **2017**, *27* (5), 1–9. https://doi.org/10.1002/adfm.201604754.

(2) Ye, H.; Lin, M.; Basaran, C. Failure Modes and FEM Analysis of Power Electronic Packaging. *Adv. Electron. Packag.* **2001**, *1*, 417–428.

(3) Han, J.; Du, G.; Gao, W.; Bai, H. An Anisotropically High Thermal Conductive Boron Nitride/Epoxy Composite Based on Nacre-Mimetic 3D Network. *Adv. Funct. Mater.* **2019**, *29* (13), 1–9. https://doi.org/10.1002/adfm.201900412.

(4) Cui, H. wang; Li, D. sheng; Fan, Q. Using Nano Hexagonal Boron Nitride Particles and Nano Cubic Silicon Carbide Particles to Improve the Thermal Conductivity of Electrically Conductive Adhesives. *Electron. Mater. Lett.* **2013**, *9* (1), 1–5. https://doi.org/10.1007/s13391-012-2114-y.

(5) Qian, R.; Yu, J.; Wu, C.; Zhai, X.; Jiang, P. Alumina-Coated Graphene Sheet Hybrids for Electrically Insulating Polymer Composites with High Thermal Conductivity. *RSC Adv.* **2013**, *3* (38), 17373–17379. https://doi.org/10.1039/c3ra42104j.

(6) Donnay, M.; Tzavalas, S.; Logakis, E. Boron Nitride Filled Epoxy with Improved Thermal Conductivity and Dielectric Breakdown Strength. *Compos. Sci. Technol.* **2015**, *110*, 152–158. https://doi.org/10.1016/j.compscitech.2015.02.006.

(7) Sadej, M.; Gojzewski, H.; Gajewski, P.; Vancso, G. J.; Andrzejewska, E. Photocurable Acrylate-Based Composites with Enhanced Thermal Conductivity Containing Boron and Silicon Nitrides. *Express Polym. Lett.* **2018**, *12* (9), 790–807. https://doi.org/10.3144/expresspolymlett.2018.68.

(8) Li, Y.; Wong, C. P. Recent Advances of Conductive Adhesives as a Lead-Free Alternative in Electronic Packaging: Materials, Processing, Reliability and Applications. *Mater. Sci. Eng. R Reports* **2006**, *51* (1–3), 1–35. https://doi.org/10.1016/j.mser.2006.01.001.

(9) Yao, Y.; Zeng, X.; Guo, K.; Sun, R.; Xu, J. Bin. The Effect of Interfacial State on the Thermal Conductivity of Functionalized Al2O3 Filled Glass Fibers Reinforced Polymer Composites. *Compos. Part A Appl. Sci. Manuf.* **2015**, *69*, 49–55. https://doi.org/10.1016/j.compositesa.2014.10.027.

(10) Wang, X. Bin; Weng, Q.; Wang, X.; Li, X.; Zhang, J.; Liu, F.; Jiang, X. F.; Guo, H.; Xu, N.; Golberg, D.; Bando, Y. Biomass-Directed Synthesis of 20 g High-Quality Boron Nitride Nanosheets for Thermoconductive Polymeric Composites. *ACS Nano* **2014**, *8* (9), 9081–9088. https://doi.org/10.1021/nn502486x.

(11) Li, Q.; Guo, Y.; Li, W.; Qiu, S.; Zhu, C.; Wei, X.; Chen, M.; Liu, C.; Liao, S.; Gong, Y.; Mishra, A. K.; Liu, L. Ultrahigh Thermal Conductivity of Assembled Aligned Multilayer Graphene/Epoxy Composite. *Chem. Mater.* **2014**, *26* (15), 4459–4465. https://doi.org/10.1021/cm501473t.

(12) Tanaka, T.; Wang, Z.; Iizuka, T.; Kozako, M.; Ohki, Y. With Sufficient Dielectric Breakdown Strength. **2011**, 3–6.

(13) Xu, Y.; Chung, D. D. L. Increasing the Thermal Conductivity of Boron Nitride and Aluminum Nitride Particle Epoxy-Matrix Composites by Particle Surface Treatments. *Compos. Interfaces* **2000**, *7* (4), 243–256. https://doi.org/10.1163/156855400750244969.

(14) Gu, J.; Zhang, Q.; Dang, J.; Xie, C. Thermal Conductivity Epoxy Resin Composites Filled with Boron Nitride. *Polym. Adv. Technol.* **2012**, *23* (6), 1025–1028. https://doi.org/10.1002/pat.2063.

(15) Goldin, N.; Dodiuk, H.; Lewitus, D. Enhanced Thermal Conductivity of Photopolymerizable Composites Using Surface Modified Hexagonal Boron Nitride Fillers. *Compos. Sci. Technol.* **2017**, *152*, 36–45. https://doi.org/10.1016/j.compscitech.2017.09.001.

(16) Sangermano, M.; Razza, N.; Graham, G.; Barandiaran, I.; Kortaberria, G. Electrically Insulating Polymeric Nanocomposites with Enhanced Thermal Conductivity by Visible-Light Curing of Epoxy–Boron Nitride Nanotube Formulations. *Polym. Int.* **2017**, *66* (12), 1935–1939. https://doi.org/10.1002/pi.5479.

(17) Pu, Z.; Mark, J. E.; Jethmalani, J. M.; Ford, W. T. Effects of Dispersion and Aggregation of Silica in the Reinforcement of Poly(Methyl Acrylate) Elastomers. *Chem. Mater.* **1997**, *9* (11), 2442–2447. https://doi.org/10.1021/cm970210j.

(18) Zhou, T.; Wang, X.; Liu, X.; Xiong, D. Improved Thermal Conductivity of Epoxy Composites Using a Hybrid Multi-Walled Carbon Nanotube/Micro-SiC Filler. *Carbon N. Y.* **2010**, *48* (4), 1171–1176. https://doi.org/10.1016/j.carbon.2009.11.040.

(19) Cho, H. B.; Tu, N. C.; Fujihara, T.; Endo, S.; Suzuki, T.; Tanaka, S.; Jiang, W.; Suematsu, H.; Niihara, K.; Nakayama, T. Epoxy Resin-Based Nanocomposite Films with Highly Oriented BN Nanosheets Prepared Using a Nanosecond-Pulse Electric Field. *Mater. Lett.* **2011**, *65* (15–16), 2426–2428. https://doi.org/10.1016/j.matlet.2011.05.005.

(20) Lin, Z.; Mcnamara, A.; Liu, Y.; Moon, K. sik; Wong, C. P. Exfoliated Hexagonal Boron Nitride-Based Polymer Nanocomposite with Enhanced Thermal Conductivity for Electronic Encapsulation. *Compos. Sci. Technol.* **2014**, *90*, 123–128. https://doi.org/10.1016/j.compscitech.2013.10.018.

(21) Hong, J. P.; Yoon, S. W.; Hwang, T.; Oh, J. S.; Hong, S. C.; Lee, Y.; Nam, J. Do. High Thermal Conductivity Epoxy Composites with Bimodal Distribution of Aluminum Nitride and Boron Nitride Fillers. *Thermochim. Acta* **2012**, *537*, 70–75. https://doi.org/10.1016/j.tca.2012.03.002.

(22) Zhang, W.; Yang, H.; Liu, F.; Chen, T.; Hu, G.; Guo, D.; Hou, Q.; Wu, X.; Su, Y.; Wang, J. Molecular Interactions between DOPA and Surfaces with Different Functional Groups: A Chemical Force Microscopy Study. *RSC Adv.* **2017**, *7* (52), 32518–32527. https://doi.org/10.1039/c7ra04228k.

(23) Liu, H.; Ye, H.; Zhang, Y.; Tang, X. Preparation and Characterization of Poly(Trimethylolpropane Triacrylate)/Flaky Aluminum Composite Particle by in Situ Polymerization. *Dye. Pigment.* **2008**, *79* (3), 236–241. https://doi.org/10.1016/j.dyepig.2008.03.001.

(24) Khan, M. A.; Shehrzade, S.; Masudul Hassan, M. Effect of Alkali and Ultraviolet (UV) Radiation Pretreatment on Physical and Mechanical Properties of 1,6-Hexanediol Diacrylate-Grafted Jute Yarn by UV Radiation. *J. Appl. Polym. Sci.* **2004**, *92* (1), 18–24. https://doi.org/10.1002/app.13593.

(25) Ko, T. -M; Cooper, S. L. Surface Properties and Platelet Adhesion Characteristics of Acrylic Acid and Allylamine Plasma-treated Polyethylene. *J. Appl. Polym. Sci.* **1993**, *47* (9), 1601–1619. https://doi.org/10.1002/app.1993.070470908.

(26) Lindner, A.; Lestriez, B.; Mariot, S.; Creton, C.; Maevis, T.; Lühmann, B.; Brummer, R. Adhesive and Rheological Properties of Lightly Crosslinked Model Acrylic Networks. *J. Adhes.* **2006**, *82* (3), 267–310. https://doi.org/10.1080/00218460600646594.

(27) Zhang, L.; Deng, H.; Fu, Q. Recent Progress on Thermal Conductive and Electrical Insulating Polymer Composites. *Compos. Commun.* **2018**, *8* (November 2017), 74–82. https://doi.org/10.1016/j.coco.2017.11.004.

(28) Peykova, Y.; Lebedeva, O. V.; Diethert, A.; Müller-Buschbaum, P.; Willenbacher, N. Adhesive Properties of Acrylate Copolymers: Effect of the Nature of the Substrate and Copolymer Functionality. *Int. J. Adhes. Adhes.* **2012**, *34*, 107–116. https://doi.org/10.1016/j.ijadhadh.2011.12.001.

(29) Gu, J.; Yang, X.; Lv, Z.; Li, N.; Liang, C.; Zhang, Q. Functionalized Graphite Nanoplatelets/Epoxy Resin Nanocomposites with High Thermal Conductivity. *Int. J. Heat Mass Transf.* **2016**, *92*, 15–22. https://doi.org/10.1016/j.ijheatmasstransfer.2015.08.081.

(30) Kostoglou, N.; Polychronopoulou, K.; Rebholz, C. Thermal and Chemical Stability of Hexagonal Boron Nitride (h-BN) Nanoplatelets. *Vacuum* **2015**, *112*, 42–45. https://doi.org/10.1016/j.vacuum.2014.11.009.

(31) Kumar, R.; Mishra, A.; Sahoo, S.; Panda, B. P.; Mohanty, S.; Nayak, S. K. Epoxy-Based Composite Adhesives: Effect of Hybrid Fillers on Thermal Conductivity, Rheology, and Lap Shear Strength. *Polym. Adv. Technol.* **2019**, *30* (6), 1365–1374. https://doi.org/10.1002/pat.4569.

(32) Moriche, R.; Prolongo, S. G.; Sánchez, M.; Jiménez-Suárez, A.; Chamizo, F. J.; Ureña, A. Thermal Conductivity and Lap Shear Strength of GNP/Epoxy Nanocomposites Adhesives. *Int.*

J. Adhes. Adhes. **2016**, *68*, 407–410. https://doi.org/10.1016/j.ijadhadh.2015.12.012.

(33) Severijns, C.; de Freitas, S. T.; Poulis, J. A. Susceptor-Assisted Induction Curing Behaviour of a Two Component Epoxy Paste Adhesive for Aerospace Applications. *Int. J. Adhes. Adhes.* **2017**, *75* (February), 155–164. https://doi.org/10.1016/j.ijadhadh.2017.03.005.

(34) Xu, Y.; Wang, X.; Zhou, J.; Song, B.; Jiang, Z.; Lee, E. M. Y.; Huberman, S.; Gleason, K. K.; Chen, G. Molecular Engineered Conjugated Polymer with High Thermal Conductivity. *Sci. Adv.* **2018**, *4* (3), 1–7. https://doi.org/10.1126/sciadv.aar3031.

(35) Zhang, L.; Ruesch, M.; Zhang, X.; Bai, Z.; Liu, L. Tuning Thermal Conductivity of Crystalline Polymer Nanofibers by Interchain Hydrogen Bonding. *RSC Adv.* **2015**, *5* (107), 87981–87986. https://doi.org/10.1039/c5ra18519j.

Acknowledgements

I would like to express my sincere gratitude to the people who helped and supported me throughout the completion of my master's degree. To the various members of IPCL whom I had the pleasure of working with over the last few years, thank you for all the fun times and the support you've given me from the time I was an intern to the two years I spent as a graduate student. I would like to thank my advisor, Prof. Dong Woog Lee, for his guidance through various research topics for the last three and a half years. I would also like to thank the committee members, Prof. So Youn Kim and Prof. Hak-Sun Kim, for taking time out of their busy schedules for the thesis defense and for their insightful comments and suggestions. To my friends, thank you for all the good memories we shared during my stay at UNIST. Finally, to my family, who always encouraged me to pursue my interests, and who helped and supported me through various situations, thank you for always being there for me.